

UC Davis

UC Davis Previously Published Works

Title

Cyanobacteriochrome-based photoswitchable adenylyl cyclases (cPACs) for broad spectrum light regulation of cAMP levels in cells

Permalink

<https://escholarship.org/uc/item/95w828pb>

Journal

Journal of Biological Chemistry, 293(22)

ISSN

0021-9258

Authors

Blain-Hartung, Matthew

Rockwell, Nathan C

Moreno, Marcus V

et al.

Publication Date

2018-06-01

DOI

10.1074/jbc.ra118.002258

Copyright Information

This work is made available under the terms of a Creative Commons Attribution License, available at <https://creativecommons.org/licenses/by/4.0/>

Peer reviewed



Cyanobacteriochrome-based photoswitchable adenylyl cyclases (cPACs) for broad spectrum light regulation of cAMP levels in cells

Received for publication, February 5, 2018, and in revised form, April 2, 2018. Published, Papers in Press, April 9, 2018, DOI 10.1074/jbc.RA118.002258

Matthew Blain-Hartung[‡], Nathan C. Rockwell[‡], Marcus V. Moreno[‡], Shelley S. Martin[‡], Fei Gan^{§1},
Donald A. Bryant^{§¶}, and J. Clark Lagarias^{‡2}

From the [‡]Department of Molecular and Cellular Biology, University of California, Davis, California 95616, the [§]Department of Biochemistry and Molecular Biology, The Pennsylvania State University, University Park, Pennsylvania 16802, and the [¶]Department of Chemistry and Biochemistry, Montana State University, Bozeman, Montana 59717

Edited by Joseph M. Jez

Class III adenylyl cyclases generate the ubiquitous second messenger cAMP from ATP often in response to environmental or cellular cues. During evolution, soluble adenylyl cyclase catalytic domains have been repeatedly juxtaposed with signal-input domains to place cAMP synthesis under the control of a wide variety of these environmental and endogenous signals. Adenylyl cyclases with light-sensing domains have proliferated in photosynthetic species depending on light as an energy source, yet are also widespread in nonphotosynthetic species. Among such naturally occurring light sensors, several flavin-based photoactivated adenylyl cyclases (PACs) have been adopted as optogenetic tools to manipulate cellular processes with blue light. In this report, we report the discovery of a cyanobacteriochrome-based photoswitchable adenylyl cyclase (cPAC) from the cyanobacterium *Microcoleus sp. PCC 7113*. Unlike flavin-dependent PACs, which must thermally decay to be deactivated, cPAC exhibits a bistable photocycle whose adenylyl cyclase could be reversibly activated and inactivated by blue and green light, respectively. Through domain exchange experiments, we also document the ability to extend the wavelength-sensing specificity of cPAC into the near IR. In summary, our work has uncovered a cyanobacteriochrome-based adenylyl cyclase that holds great potential for the design of bistable photoswitchable adenylyl cyclases to fine-tune cAMP-regulated processes in cells, tissues, and whole organisms with light across the visible spectrum and into the near IR.

Class III adenylyl cyclases generate the ubiquitous second messenger cAMP from ATP often in response to chemical or environmental signals. In prokaryotes, cAMP frequently partners with the catabolite activator protein to regulate energy metabolism (1, 2), and also regulates motility and virulence (3). In eukaryotes, cAMP levels control crucial processes such as chromosome segregation, gene expression, and cellular metabolism (4). This regulatory plasticity arises from juxtaposition of adenylyl cyclase catalytic domains with a wide variety of “input” domains that sense different chemicals, nutrients, light, physical signals, and pH. Despite the signal input diversity, the protein-fold of homodimeric Class III adenylyl cyclase catalytic domains (termed cyclase homology domains (CHD))³ and a catalytic mechanism that requires participation of two subunits across a dimer interface have been preserved from prokaryotes to eukaryotes for billions of years (5).

Cyanobacterial phototrophs possess a diverse complement of adenylyl cyclases that have been shown to regulate respiration (6), motility (7, 8), and heterocyst formation (9). Although blue light (B)-sensing adenylyl cyclases that utilize flavin are present in some cyanobacteria (10, 11), cyanobacterial adenylyl cyclases typically lack photoreceptor domains and those known to be under light control are indirectly regulated by other photoreceptors (12, 13). The cyanobacterial species *Microcoleus sp. PCC 7113* contains one of the largest complements of adenylyl cyclase genes with sensor regions recognized as a phospho-accepting response regulator, a heme containing NO-sensor, a ligand-binding periplasmic sensor, and one cGMP-specific phosphodiesterases/cyanobacterial adenylyl cyclases/formate hydrogen lyase transcription activator Fh1A (GAF) domain sensor. GAF domains often mediate ligand-dependent protein–protein interactions; one of these adenylyl cyclase genes, *i.e.* MIC7113_2205 contains a GAF domain similar to those found

This work was supported by grants from the Chemical Sciences, Geosciences, and Biosciences Division, Office of Basic Energy Sciences, Office of Science, United States Department of Energy Grant DOE DE-FG02-09ER16117 (to J. C. L.), National Science Foundation Grant MCB-1613022 (to D. A. B.), and National Institutes of Health, NIGMS Grant T32-GM07377 (to M. B.-H.). The authors declare that they have no conflicts of interest with the contents of this article. The content is solely the responsibility of the authors and does not necessarily represent the official views of the National Institutes of Health.

This article contains Table S1 and Figs. S1–S9.

¹ Present address: The Scripps Research Institute, S202, 10550 North Torrey Pines Rd., La Jolla, CA 92037.

² To whom correspondence should be addressed: 1 Shields Ave., Davis, CA 95616. Tel.: 530-752-1865; E-mail: jclagarias@ucdavis.edu.

³ The abbreviations used are: CHD, cyclase homology domain; AC, adenylate cyclase; B, blue light; Bc, continuous blue light; BLUF, sensors of blue-light using FAD; BV, biliverdin IX α ; CBCR, cyanobacteriochrome; DXCF, Asp-Xaa-Cys-Phe; G, green light; Gc, continuous green light; Rc, continuous red light; PAC, photoactivated adenylate cyclase; cPAC, cyanobacteriochrome photoswitchable adenylate cyclase; PCB, phycocyanobilin; PEB, phycoerythrobilin; RP-HPLC, reverse phase-high performance liquid chromatography; SEC, size exclusion chromatography; IPTG, isopropyl 1-thio- β -D-galactopyranoside; X-Gal, 5-bromo-4-chloro-3-indolyl β -D-galactoside; β -gal, β -galactosidase; REC, response regulator; PAS, Per/Arnt/Sim.

Cyanobacterial photoactivatable adenylyl cyclases

in cyanobacteriochrome (CBCR) photoreceptors, distant relatives of red/far-red sensing plant phytochromes (14).

CBCRs possess heme-derived, linear-tetrapyrrole (bilin)-binding GAF domains that can perceive the complete range of the visible light spectrum, extending into the near UV and the near IR (14–16). All CBCRs utilize phycocyanobilin (PCB) that is spectrally tuned by key residues within the GAF domain scaffold (17–26). MIC7113_2205 belongs to the DXCF subfamily of CBCRs, characterized by two conserved cysteine residues, each of which can form covalent linkages to the PCB precursor to alter the π -conjugated chromophoric system to absorb blue light (18, 27). Although CBCRs are typically associated with histidine kinase, methyl chemotaxis, and cyclic di-GMP regulatory GGDEF or EAL output domains, MIC7113_2205 is the first adenylyl cyclase (Fig. S1) to be identified with a putative light-sensing CBCR GAF domain. MIC7113_2205 also contains an N-terminal response regulator (REC) and Per/Arnt/Sim (PAS) domains, both of which could represent additional input domains for other chemical or physical signaling systems. Atypical for widespread adenylyl cyclases with unrelated GAF domains, this novel adenylyl cyclase-associated CBCR gene appears unique to this *Microcoleus* species. The observation that the related cyanobacterium *Microcoleus chthonoplastes* PCC 7420 possesses a flavin-based, B-regulated adenylyl cyclase (10) suggests that light-regulation of cAMP production may be particularly critical for cyanobacteria in this genus.

The ability to manipulate adenylyl cyclase activity with light enables precise spatial and temporal control of cAMP levels within cells, organs, and tissues. Indeed, genetically-encoded photoactivated adenylyl cyclases (PAC) with Blue-Light sensors Using FAD (BLUF) domains, such as EuPAC, bPAC, BgPACs, LiPAC, NaPACs, and OaPAC (11, 28–38), or with flavin-binding LOV domains, such as mPAC (10), have been successfully deployed in mammalian cells. The utility of bilin-based PACs for similar applications was first documented by Gomelsky and co-workers (39), who fused a biliverdin IX α (BV)-dependent bacteriophytochrome to an adenylyl cyclase catalytic domain that could be reversibly controlled with red and far-red light (Fig. 1). As optogenetic tools, bistable phytochrome-based PACs offer the advantage that two wavelengths of light can be used to reversibly regulate cAMP production in cells in real time, rather than relying on thermal reversion pathways to inactivate the photoactivated state, e.g. for flavin-based PACs. Because of the small size of CBCR input domains (~200 amino acids), and extended spectral range, CBCR-based adenylyl cyclases hold particular promise as optogenetic reagents.

The present work was undertaken to test the hypothesis that MIC7113_2205 functions as a light-regulated adenylyl cyclase and to characterize the molecular basis of its light regulation. Our studies show that MIC7113_2205 is a bistable, blue/green (B/G)-regulated adenylyl cyclase that we hereafter refer to as cPAC for cyanobacteriochrome-based Photoswitchable Adenylyl Cyclase. We also test the interchangeability of CBCR GAF domains to alter the wavelength specificity of cPAC for its photoswitchable cAMP regulation *in vivo*, providing a roadmap for spectral engineering of a versatile new family of CBCR-based optogenetic actuators.

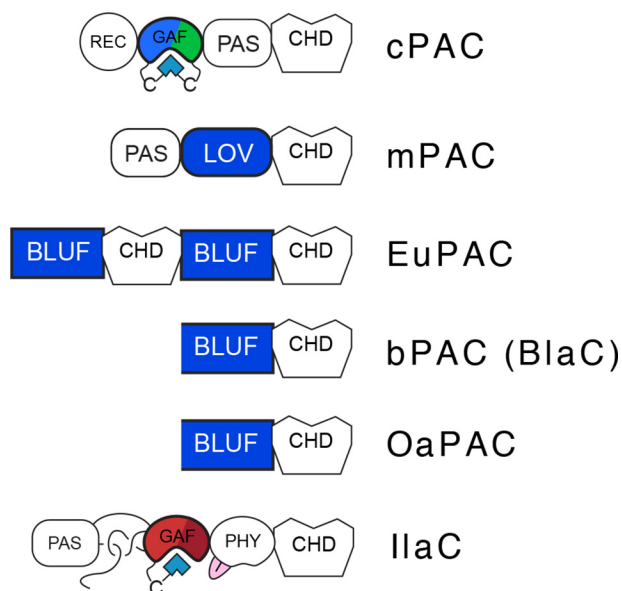


Figure 1. cPAC is a cyanobacterial photoactivated adenylyl cyclase. Shown are domain architectures of cPAC compared with those of other characterized PACs.

Results

cPAC is a bistable blue/green sensor

To analyze the photochemical properties of cPAC, we expressed a synthetic full-length cPAC gene in an *Escherichia coli* strain engineered to produce PCB from endogenous heme, and the recombinant holoprotein was purified as described previously (19, 40). In the dark-adapted P_b state, the PCB chromophore of cPAC adopted a 15Z configuration with an absorbance maximum at 410 nm in the B spectral region. Upon exposure to saturating B light, the chromophore photoconverted to its 15E configuration with an absorbance maximum at 520 nm in the G spectral region (Fig. 2A). P_g could be fully photoconverted to the B-absorbing P_b form with saturating G light. The B/G spectral properties of cPAC were consistent with those of other two-cysteine CBCRs in the DXCF subfamily, and its specific absorption ratio value of 0.18 indicated near saturated binding of PCB to the apoprotein (18, 19, 41). Dark reversion of cPAC was found to be slow on the timescale of biochemical assays, with $\leq 5\%$ change over 90 min (Fig. S2A). Moreover, the difference spectrum for dark reversion did not match that for photoconversion (Fig. S2B). This difference indicates that other processes are occurring on the same timescale, such as changes in chromophore content (19) or oxidation of the DXCF Cys (42), making it likely that regeneration of the blue-absorbing 15Z dark state is overestimated by this approach. Taken together with the linearity of cPAC in AC assays lasting 60 min (Fig. 2B), it is clear that dark reversion is not a confounding factor in our experiments.

cPAC is a photoswitchable adenylyl cyclase

The C-terminal region of cPAC (MIC7113_2205) is annotated in GenBankTM as an “adenylyl or guanylyl cyclase domain.” Further sequence analysis supports designation of cPAC as an adenylyl cyclase as both key adenosine-specific binding residues in the active site as well as all key metal and

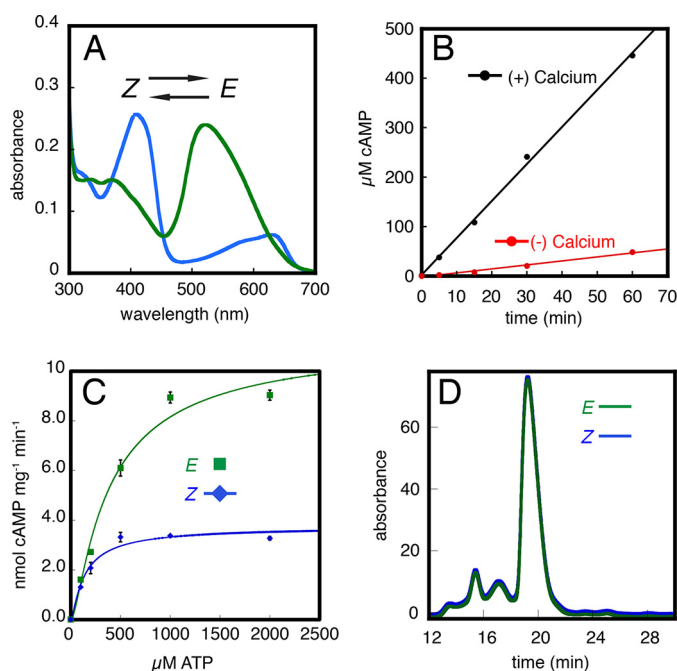


Figure 2. cPAC is blue/green photoswitchable adenylyl cyclase. *A*, spectra of cPAC displays the distinct B-absorbing (15Z) photostate and the G-absorbing (15E) photostate. *B*, time course assay of production of cAMP by the G-absorbing 15E state of cPAC with or without calcium present in the media. *C*, initial rate kinetics of cPAC in the 15E and 15Z photostates. Data are fit to a second order fit derived from the Michaelis-Menten equation: $V_o = (V_{max}[S]^2)/(k^2 + 2k[S] + [S]^2)$. *D*, HPLC-SEC trace of full-length cPAC in the 15E and 15Z states. The major peak elutes at 19.6 min.

transition state residues are present (31, 43) (Fig. S1). To resolve whether cPAC is an adenylyl or guanylyl cyclase, the activity of the 15Z- P_b and 15E- P_g states were compared using Mg-ATP or Mg-GTP as substrate. cPAC was able to convert Mg-ATP to cAMP (Fig. 2B); however, no cGMP was detected by reverse phase-HPLC (RP-HPLC) when Mg-GTP was used as substrate. The 15E- P_g state also produced more cAMP than the 15Z- P_b state indicating that cPAC is light regulated. In view of the cyanobacterial adenylyl cyclase literature, we next tested whether cPAC activity was affected by addition of calcium or bicarbonate. These studies showed that 5 mM calcium greatly increased the activity of cPAC in both 15Z- P_b and 15E- P_g states (Fig. S3A). For the more active 15E- P_g state, the presence of calcium resulted in a >10-fold greater cAMP accumulation compared to reaction mixtures lacking added calcium (Fig. 2B). By contrast, cPAC activity was stimulated only slightly (~2.5-fold) by the addition of 50 mM bicarbonate, nor did bicarbonate further stimulate cPAC activity more than calcium alone (Fig. S3B). This indicates that Ca^{2+} could stimulate cPAC activity *in vivo*, but probably it is not regulated by bicarbonate.

Initial rate measurements for both E and Z states of cPAC were next performed as a function of Mg-ATP concentration in the optimized buffer medium (Fig. 2C). A modified Michaelis-Menten analysis using a second-order reaction model fit the data slightly better than the standard analysis (44) (Fig. S4A, Table S1). The specific activity of cPAC in the 15Z- P_b dark state was estimated to be 3.8 nmol of cAMP $min^{-1} mg^{-1}$, whereas that of the 15E- P_g active state was estimated to be 11.4 nmol of cAMP $min^{-1} mg^{-1}$. These specific activities are comparable with those of flavin-based adenylyl cyclases in the activated

Table 1

Activity comparison of cPAC and flavin binding PACs

cPAC specific activity was measured as described under "Experiment procedures." Enzyme activity data points were analyzed in triplicate, and S.D. was calculated.

| Adenylyl cyclase | Specific activity | |
|-------------------|------------------------------|------------------|
| | Activated state | Dark state |
| | nmol cAMP $min^{-1} mg^{-1}$ | |
| cPAC | 11.4 ± 0.5 | 3.8 ± 0.2 |
| bPac | 10 ± 2 | 0.03 ± 0.005 |
| OaPac | 9 ± 1 | 0.5 ^a |
| mPac | 30 ± 20 | 1.0 ± 0.6 |
| EuPac | 3.5 | 0.3 ^a |
| BlaC ^b | 57 | 0.5 ^a |

^a Data not reported: estimated value from enzymatic data.

^b BlaC and bPac are the same protein, but were analyzed and documented separately (30, 31).

state (Table 1). As has been seen previously for other soluble adenylyl cyclases (45), cPAC turnover was substrate inhibited at high Mg-ATP concentrations (Fig. S4B).

The REC domain is necessary for cPAC activity

To analyze how the domain architecture of cPAC affects its activity, several truncations were constructed. The first two of these, cPAC(Δ R2) and cPAC(Δ R3), lacked the N-terminal REC domain, while retaining two or three predicted helices at the N terminus of the GAF domain, respectively. Two of these helices are typically found necessary for proper GAF domain folding. Two other constructs, cPAC(Δ RG) lacked both the REC and GAF domains, whereas the cPAC(Δ RGP) construct contained only the cyclase domain (Fig. S5A). Truncated cPAC(Δ R2) and cPAC(Δ R3) proteins were both folded and photoactive, exhibiting P_b and P_g spectra nearly indistinguishable from those of the full-length cPAC (Fig. 2A and Fig. S5). By contrast, adenylyl cyclase activities of these and all truncated cPAC constructs were less than 5% of WT, and adenylyl cyclase activities of cPAC(Δ RG) and cPAC(Δ RGP) were barely detectable (Fig. 3A). It is also interesting that the two REC-less constructs cPAC(Δ R2) and cPAC(Δ R3) did retain some light-regulated adenylyl cyclase activity although the significance of the differences is unclear due to their low AC activities. Taken together, these data indicated that the REC domain is critical for cPAC activity in either state.

The regulatory activity of REC domains of two-component response regulator proteins is typically modulated by phosphorylation. REC domain phosphorylation could affect the monomer-dimer equilibrium of canonical response regulator proteins to influence, *e.g.* their DNA-binding affinity, and/or could affect the conformation/dynamics/activity of other associated output domains (46). To test the first possibility, full-length cPAC and all four truncated constructs were analyzed by HPLC-size exclusion chromatography (HPLC-SEC). As seen in Fig. 2D, full-length cPAC migrates as a dimer in both 15Z- P_b and 15E- P_g states (Table 2). By contrast, all truncated cPAC constructs appear monomeric under these conditions (Table 2, Fig. S6); these results suggest that the REC domain is critical for homodimer formation, which in turn is necessary for cPAC catalytic activity.

We next examined whether the P_b to P_g photoconversion could affect the quaternary state of the protein. As shown in Fig.

Cyanobacterial photoactivatable adenyl cyclases

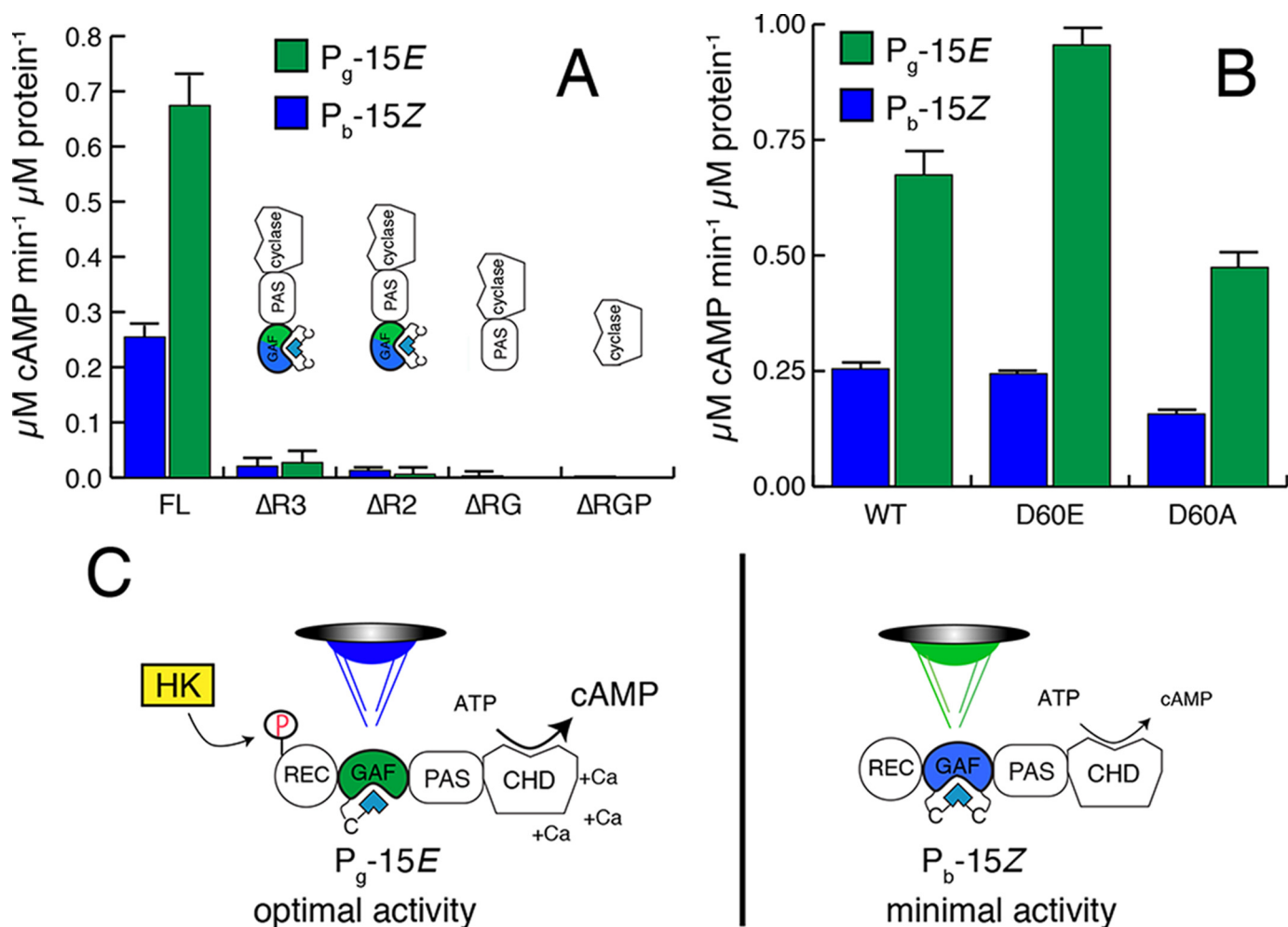


Figure 3. REC domain of cPAC is essential for optimal activity. *A*, bar graph of enzyme activity of full-length cPAC and subsequent domain truncations. $\Delta R3$ and $\Delta R2$ denote truncation of the REC domain leaving 3 or 2 helices of the N-terminal GAF domain, respectively, ΔRG denotes the construct of the PAS–cyclase domain and ΔRGP denotes only the cyclase domain (see text for details). *B*, bar graph of enzyme activity comparing WT cPAC to cPAC(D60E) and cPAC(D60A) mutations. *C*, schematic of optimal activity conditions for cPAC (B light triggering the 15E- P_g state, phosphorylation of the REC domain in the presence of 5 mM Ca^{2+}) as compared with conditions for minimal activity (G light triggering the 15Z- P_b state, with buffer lacking Ca^{2+}).

Table 2

Predicted size and oligomeric state of cPAC and truncated variants

HPLC-SEC measurements were performed in duplicate ($n = 2$) and predicted molecular weight averaged as described under “Experimental procedures.”

| Construct | HPLC-SEC measurement | Predicted monomer molecular mass |
|----------------------|----------------------|----------------------------------|
| cPAC (full-length) | 143 \pm 8 kDa | 77 kDa |
| cPAC($\Delta R3$) | 68 \pm 5 kDa | 60 kDa |
| cPAC($\Delta R2$) | 66 \pm 4 kDa | 58 kDa |
| cPAC(ΔRG) | 45 \pm 4 kDa | 41 kDa |
| cPAC(ΔRGP) | 30 \pm 2 kDa | 27 kDa |

2D, the HPLC-SEC elution profiles of both states of full-length cPAC were superimposable. Based on this result, we conclude that photoactivation of cPAC does not lead to a major change in overall protein conformation. This also implies that small light-induced structural changes are responsible for the regulation of activity of cPAC, a result similar to that reported for BLUF containing PACs (11, 37, 38). Our HPLC-SEC data also suggests that homodimerization is required for efficient catalytic turnover. However, dimerization is not required for the cPAC photocycle, because both cPAC($\Delta R2$) and cPAC($\Delta R3$) constructs retained the same spectral properties as the full-length protein (Fig. S5C). As all truncated proteins are monomeric, the

enzyme activity data suggest that REC domain dimerization restricts conformational sampling of CHD domains that disfavor formation of the catalytically competent dimer or, alternatively, that REC-dependent dimerization is necessary to increase the local CDH concentration to support dimerization and catalytic turnover (5).

cPAC activity is modulated by REC domain phosphorylation

Because the REC domain is required for cPAC function, we next performed experiments to test the role of REC domain phosphorylation on its catalytic activity. The transmitter kinase responsible for its phosphorylation is unknown, so we constructed site-directed variants of the conserved predicted phospho-accepting Asp-60 residue of cPAC (as categorized for a REC domain consensus sequence, CDD 238088) to mimic its phosphorylated and nonphosphorylated states (47). To do so, we introduced phosphomimetic D60E “gain-of-function” and D60A “loss-of-function” substitutions; such functional substitutions have been described in the response regulator receiver family previously (48–50). Both cPAC variants exhibited photochemical properties identical with those of the WT (Fig. S5C), demonstrating that these substitutions did not perturb

the structure or light-sensing function of the CBCR GAF domain of cPAC. Surprisingly, the 15E-P_g state of D60E exhibited 150% AC activity of the WT; by comparison, the 15E-P_g state of D60A was 30% less active than the WT. However, the activities of the 15Z-P_b states of WT and D60E mutant were nearly identical (Fig. 3B), suggesting that phosphorylation selectively enhances the activity of the photoproduct state. This conclusion must be tempered by the possibility that the 15Z-P_b state of WT cPAC from *E. coli* may already be partially phosphorylated when isolated. Taken together, our data suggest that phosphorylation of the REC domain likely plays a regulatory role on cPAC activity *in vivo*. The interplay between REC phosphorylation and light activation of the GAF domain remains an interesting subject for future study. Taken together, our enzyme data indicate that the maximum signal output from cPAC is achieved following B light treatment, when the REC domain is phosphorylated and calcium levels are elevated (Fig. 3C).

In vivo light-regulated manipulation of cAMP levels by cPAC

To test the efficacy of cPAC as an optogenetic tool *in vivo*, we co-expressed cPAC with a PCB biosynthetic plasmid in *cya*⁻ *E. coli* strain VJS711 that lacks endogenous adenylyl cyclase activity (51). This strain allows us to measure the cAMP-dependent activation of the endogenous β -gal (*lacZ*) gene via the plasmid-derived cPAC without interference of endogenous CYA-dependent cAMP production. When spread on LB plates containing X-Gal/IPTG, only strains that produce sufficient levels of cAMP will appear blue (Fig. 4A). Indeed, cell lines expressing full-length cPAC were blue on X-Gal plates, revealing the production of endogenous cAMP and its subsequent activation of β -gal expression. By contrast, the *cya*⁻ strain expressing the truncated cPAC(Δ RGP) construct failed to produce β -gal under identical conditions (Fig. S7). As expected from *in vitro* assay results, WT cPAC-expressing cultures grown under continuous blue light (Bc) possessed significantly more β -gal activity than cultures grown under continuous green light (Gc) (Fig. 4B). We expected that cPAC would modulate global cAMP levels in a heterologous system, measured via a direct cAMP assay method, as seen with previous PACs (28, 29, 31). Similar results were observed with *E. coli* liquid suspension cultures grown under Bc, which yielded significantly more cAMP (~2.5 times more) than cultures grown under G_c (Fig. 4C). Control measurements of the *cya*⁻ strain lacking cPAC revealed insignificant amounts of cAMP production. These studies confirm that cPAC retains its photoregulatory properties *in vivo*.

CBCR domain exchange yields cPAC variants with altered wavelength selectivity

CBCRs have been identified that can sense light from the near UV, throughout the visible spectra, and into the near IR (52). Because 3D structures of CBCRs so far examined are all quite similar, this suggests that substitution of different wavelength-sensing CBCRs for one another will be feasible to provide a broad array of cPAC reagents tailored for potentially any wavelength combination desired (53–55). We therefore sought to create new cPAC-based chimeras by exchanging the B/G

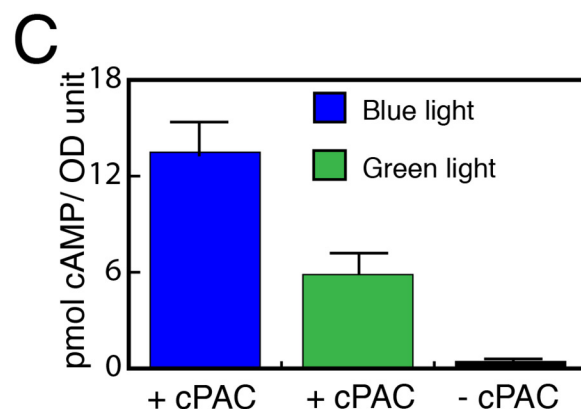
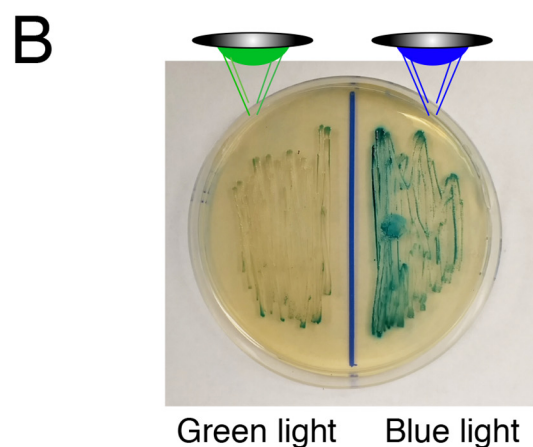
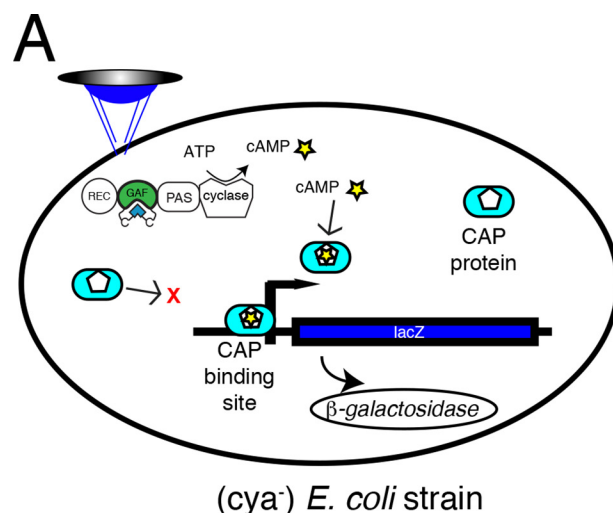


Figure 4. cPAC can modulate cAMP levels *in vivo*. A, schematic of cPAC mediating *lacZ* gene expression via modulation of cAMP levels in (*cya*⁻) *E. coli* cells. B, LB (X-Gal/IPTG) plate displaying β -gal cleavage of X-Gal in *E. coli* expressing cPAC in the section of plate exposed to Bc, whereas Gc vastly reduced X-Gal cleavage in cells. C, *in vivo* levels of cAMP in *E. coli* liquid suspension cultures expressing cPAC and incubated under Bc or Gc. cAMP levels were normalized in each culture by O.D. (600 nm) value.

CBCR GAF domain of cPAC with GAF domains from two other CBCR lineages. We chose the green/red CBCR RcaE from *Fremyella diplosiphon* (22) and a newly identified CBCR JSC1_58120g3 from *Leptolyngbya* sp. JSC1 (Fig. 5A). One of three GAF domains of a multi-GAF methyl-accepting chemotaxis transducer, *i.e.* JSC1_58120g3, is closely related to the canonical red/green family. JSC1_58120g3 is a previously unde-

Cyanobacterial photoactivatable adenylyl cyclases

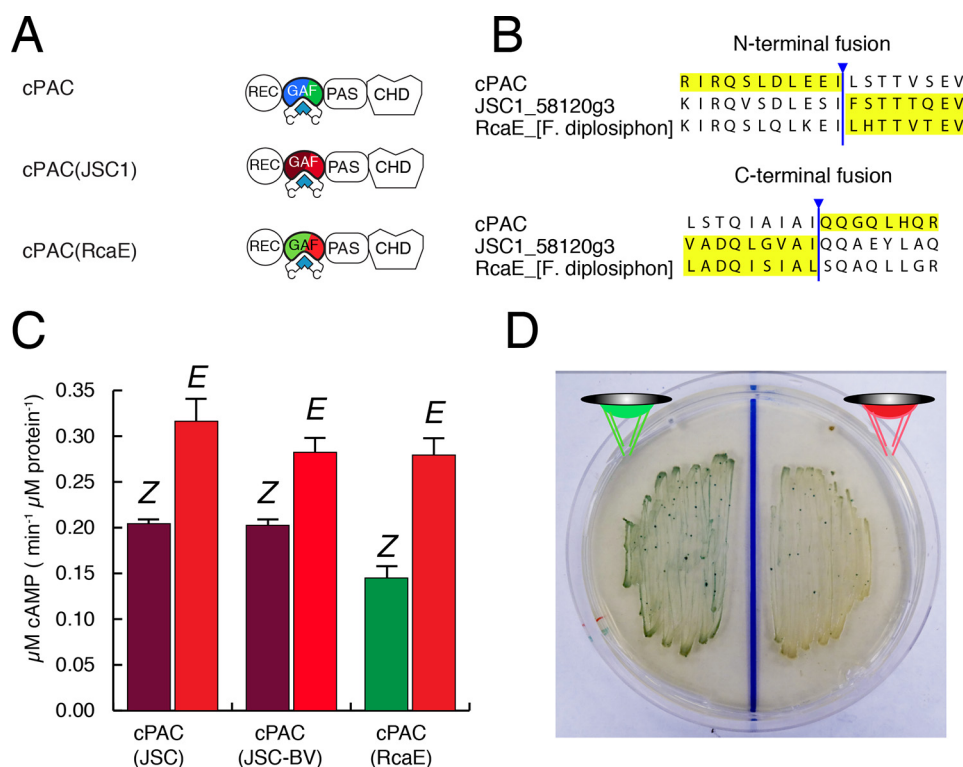


Figure 5. cPAC as a platform for multicolored fusion constructs. *A*, jellybean diagram of cPAC fusion constructs. *B*, alignment showing the N- and C-terminal fusion breakpoints for cPAC and GAF domains of JSC1_58120g3 and RcaE. *Yellow* highlight denotes residues present in the resultant fusion construct. *C*, bar graph of enzyme activity of fusion constructs in the 15E and 15Z photostates. *D*, LB plate (as described above) showing greater X-Gal cleavage and blue coloring in *E. coli* cells expressing cPAC(RcaE) that are exposed to Gc, as compared with cells exposed to Rc.

scribed CBCR found in the *Leptolyngbya* sp. JSC1 genome (56), so it was first expressed and purified as its PCB adduct for spectroscopic analysis. JSC1_58120g3 exhibited 15Z state peak absorbance of 712 nm and 15E state peak absorbance of 654 nm. Therefore, JSC1_58120g3 can be classified as a far-red/red CBCR similar, albeit unrelated to those recently described (26). JSC1_58120g3 can also utilize biliverdin (BV) as an alternative chromophore, although surprisingly, the spectral properties of the BV adduct of JSC1_58120g3 were quite similar to the PCB adduct (Fig. S8), peaking at 716 nm in its 15Z state and at 646 nm in its 15E state.

For selection of fusion junctions for these chimeras, we chose an N-terminal fusion point between charged residues in a conserved region within the first helix of the cPAC GAF domain, and a C-terminal fusion point in the C-terminal α helix in the GAF domain leading toward a highly conserved region at the N terminus of the downstream PAS domain (Fig. 5B). The resulting fusion proteins, designated cPAC(JSC1) and cPAC(RcaE), retained their donor parent CBCR photocycles (Fig. S8). Because JSC1_58120g3 binds BV as well as PCB, the BV adduct of cPAC (JSC1-BV) was examined spectrophotometrically. These measurements showed that both bilin adducts of cPAC retained the spectroscopic signature of the corresponding bilin-reconstituted JSC1_58120g3 parent, although their 15E photoproduct states of the former reverted to their 15Z dark states more rapidly than those of the parent JSC1_58120g3 constructs.

Finally, the cPAC chimeras were analyzed for adenylyl cyclase activity under similar *in vitro* assay conditions used for

WT cPAC. Although the overall cyclase activity was lower in each construct when compared with WT cPAC, both chimeras displayed differential AC activity for their 15Z and 15E states. For cPAC(RcaE), the 15E state was twice as active as its 15Z state, whereas cPAC(JSC) exhibited only a ~33% enhancement in its 15E state (Fig. 5C). A similar result was also observed for cPAC(JSC-BV). In addition, when transformed into the VJS711 *cya*⁻ strain, cPAC(RcaE) was able to activate β -gal activity under green light, whereas red light suppressed β -gal activity on agar plates (Fig. 5D). Taken together, these studies document that re-engineering new color specificity for cPACs by CBCR exchange is a viable and surprisingly facile approach. Such first-generation constructs represent promising subjects for further optimization of spectrally diverse cPAC tools for *in vivo* regulation of cAMP signaling with light.

Discussion

Cyanobacteria rely on the ability to sense environmental light conditions and therefore utilize photosensory proteins to optimize photosynthesis and regulate motility (37), processes that are influenced by levels of the second messenger cAMP. *Microcoleus* sp. PCC 7113 has one of the largest complement of adenylyl cyclase enzymes for cyanobacteria; among them is the novel cPAC light sensor described here. The many distinct sensory modules in the *Microcoleus* adenylyl cyclase family suggest that cAMP signaling participates in many processes critical for adaptation to the complex intertidal and soil sediment environments where *Microcoleus* is found (57–59). Flavin-

and retinal-based light-sensing adenylyl cyclases are notably widespread in cyanobacteria and algae (12, 30, 37, 60–62), but cPAC is the first example of an adenylyl cyclase with a CBCR input domain.

Our studies show that cPAC is differentially modulated by blue (B) and green (G) lights. Blue light-activated CBCR-based diguanylate cyclases, which trigger rapid settling to avoid photodamage of the photosynthetic apparatus at high fluences, are notably more common in cyanobacteria (23, 63). In addition, the need for B light-regulated adenylyl cyclase activity is underscored by the observation that all known PAC sensors are activated by B light. Unlike the bPAC family of BLUF-, LOV-, and retinal-based sensors, the activity of cPAC can be rapidly adjusted/reversed by G light, providing greater temporal control of cAMP signaling. Our *in vitro* studies document the bistability of cPAC and thus implicate the potential to trigger and reverse cAMP signaling *in vivo*. Beyond the scope of the present investigation, such studies necessitate construction of cell lines such as mammalian neurons or other eukaryotic cells engineered with more sophisticated reporter systems.

cPAC: An integrator of multiple signal inputs?

Well suited to play a role in light-regulated cAMP production in cyanobacteria, the complex architecture of cPAC suggests that it integrates information from multiple input signals. Indeed, our studies implicate the N-terminal REC domain as an input domain that is also required for the adenylyl cyclase activity of cPAC. cPAC was most active when its REC domain was modified to mimic its phosphorylated state, and was least active in an unphosphorylatable REC domain variant. These observations suggest that the REC domain stabilizes the homodimeric quaternary structure of full-length cPAC to enhance formation of the interdomain transition state of Type III adenylyl cyclase enzymes (5). The enhanced activity of the phosphomimic mutant may be due to further constraints on the REC domain that favor catalysis. Because the truncated constructs are essentially inactive, we propose that the REC domain may also minimize conformational sampling of the GAF, PAS, and/or CHD domains possibly by reducing unproductive conformational sampling of the homodimer. Future studies will be needed to address these hypotheses.

The cPAC gene is located immediately downstream of an ORF that encodes a histidine kinase, MIC7113_RS10675, annotated as a PAS-SsrA sensor kinase. SsrA proteins are known components of two-component systems (64), thus we speculate that MIC7113_RS10675 may be responsible for the regulation of the phosphorylation status of cPAC. This locus also has apparent orthologs in other cyanobacteria. It will be interesting to test whether cPAC phosphorylation plays a more dramatic regulatory role of the adenylyl cyclase activity compared with the phosphomimetic variant. With respect to other input signals to cPAC, bicarbonate does not appear to be a major agonist in contrast with its known regulatory role of other cyanobacterial adenylyl cyclase proteins (65–69). cPAC was greatly stimulated by the presence of calcium ions (Ca^{2+}). Because Ca^{2+} has been shown to help mediate ATP binding in adenylyl cyclase enzymes (69), changes in Ca^{2+} concentrations may also trigger

increased cAMP production by cPAC. The Ca^{2+} sensitivity of cPAC remains an important consideration for optogenetic applications going forward (see below).

cPAC as a optogenetic tool

The activity of cPAC was sufficient to trigger light-dependent differences in cAMP levels *in vivo*, as well as trigger cAMP-regulated gene expression (*lacZ*) in *E. coli* in a B/G-dependent fashion. The successful manipulation of cAMP *in vivo* by cPAC shows that this protein is a viable platform for optogenetic tool applications in a wide variety of photosynthetic species where reduced bilins, also known as phytybilins, are present. These not only includes cyanobacteria, but also eukaryotic algae and plants (70). We envisage considerable utility of this tool for light-dependent reprogramming of plastid metabolic pathways in chlorophyte algae such as *Chlamydomonas reinhardtii*, due to its ability to produce PCB despite its lack of bilin-based sensors in the phytochrome family (71).

Known PACs (with BLUF and LOV domains) have previously been shown to be effective in regulating a variety of cAMP-related processes in heterologous organisms with B light (10, 11, 29, 31, 72). An advantage of cPAC, and its variants, lies with the extensive color palette of CBCRs and the ability to interchange CBCR GAF domains that sense light from the near UV to the near IR; this contrasts with the more limited color-sensing properties of canonical phytochromes (14). Based on these attributes, CBCRs have garnered considerable interest for use as optogenetic tools in live cells (53–55, 73). The ability of CBCRs to switch rapidly between stable photostates (15E/Z) without relying on a dark or thermal reversion to reset between active and inactive states is another key feature of the cPAC family. This property enables switching between active/inactive states with supplemental light of the appropriate wavelength to trigger rapid changes in cAMP-dependent processes *in situ*.

Finally, our studies demonstrate that cPAC is a good lead compound for creation of a suite of adenylyl cyclase enzymes that respond to a variety of wavelengths. The successful fusion constructs tested here, especially cPAC(RcaE), establishes the plug-and-play modularity of the cPAC regulator that presage our ability to make robust light-responsive adenylyl cyclases that span the near UV to the NIR. Although intriguing as proof-of-concept enzymes, these proteins, along with native cPAC, are good targets for further engineering efforts. We expect that our growing understanding of CBCR structure (22, 74) will inform structure-based approaches to design new cPACs with improved signaling dynamics and dynamic range.

Applications beyond photosynthetic species

As various CBCRs bind several types of bilin chromophores, constructs can conceivably be tailored to utilize natural precursors that may be more abundant in the organism of choice. For example, although PCB is not naturally produced in nonphotosynthetic species, BV is widely distributed in nature including yeast and mammals. For this reason, biosynthesis of PCB has also been engineered into eukaryotic “chassis” organisms that naturally do not produce these compounds (75–78). Increased expression of heme oxygenases has been used to enhance the

Cyanobacterial photoactivatable adenylyl cyclases

synthesis of BV in bacterial and mammalian cells (79, 80). Indeed, bilin availability remains a critical issue to resolve for optogenetic applications because, in all cases tested, chromophore binding is critical for optimizing the dynamic range of two-color regulation by phytochrome and CBCR systems (39, 54, 81).

As shown previously, CBCRs can also be engineered to alter the dark reversion rate of the photosensory domain, which can be used to create tools that are active at a particular wavelength, and inactive in the dark (55). When combined with light-activated phosphodiesterase proteins (82), the levels of cAMP also can be tailored to precise levels, or to eliminate basal activity, in the 15Z state of cPAC and variants. We envisage a bright future for combination of these enzymes and spectrally diverse PACs for the fine-tuned control of cAMP-regulated processes in living cells using a variety of colors of light.

Experimental procedures

Protein expression and spectral analysis

The gene Mic7113_2205 (cPAC) was purchased as synthetic DNA from GenScript®. cPAC and variants were expressed as intein–chitin-binding domain fusion proteins in *E. coli* cells engineered to produce PCB using a dual plasmid system, as described previously (27, 40). Proteins were purified from *E. coli* on a chitin column (New England Biolabs) in accordance with the manufacturer's directions and characterized by SDS-PAGE (Fig. S9). Absorption spectra and dark reversion measurements for cPAC and variants were acquired as previously described (27). Photoconversion of cPAC and variants during *in vitro* calculations was verified in this manner.

In vitro cyclase assay

The BCA assay (Pierce) was used to determine protein concentration for all assays with BSA as a protein standard. The standard cyclase assay buffer was composed of 0.5 M Tris-HCl, pH 7.6, 0.05 M NaCl, 0.01 M MgCl₂, 0.5 mM EDTA. CaCl₂ was added to buffer at a final concentration of 5 mM, whereas NaHCO₃ was added at a final concentration of 50 mM. The desired concentration of GTP or ATP was added to buffer prior to reaction initiation. Purified protein (10 mM final concentration) in the 15E or 15Z states was added to initiate reaction in the dark. Photostates of protein were achieved using LEE filters (number 071 Tokyo blue and number 090 dark yellow green) as described previously (83), and confirmed via spectroscopic analysis. Assays were terminated after 1 h in the dark with addition of EDTA, pH 8.0, to a final concentration of 0.1 M. An aliquot (15 μl) of each reaction solution was injected into an Agilent 1100 series HPLC and passed through a Phenomenex® Synergi 4 μM Fusion-RP 80 Å column and Security Guard Cartridge (C18, 4 × 2 mm), under conditions previously described (83). The internal standard of cAMP (Sigma) eluted at 12.1 min. A standard curve of cAMP levels using area under peak values correlated with cAMP concentrations of 2.0 to 400 μM. All area calculations were performed using Agilent ChemStation software. All cyclase assays are performed in triplicate at room temperature (20 °C).

HPLC-SEC

Buffer used for HPLC-SEC assays was 40 mM Tris acetate, pH 8.3, 1 mM EDTA, 0.15 M NaCl. Run time was 40 min with an isocratic flow rate of 0.6 ml/min, using ThermoScientific Ultimate 3000 HPLC and a GE Superdex™ 200 Increase 10/300 GL column. Aliquots (50 μl) of purified cPAC and variants (in either 15E or 15Z states) were injected in a 100-μl loop. 15E and 15Z states were achieved as described above, and confirmed via spectroscopic analysis. Elution traces and peaks were analyzed using Chromeleon 7 software (Dionex). All runs were performed in darkness to avoid photoconversion prior to elution. Molecular weight calculations were performed via standard curve preparation, seen in supporting Fig. S4. Samples were analyzed in duplicate ($n = 2$) and the molecular weight measurements were averaged and the plus/minus spread was described.

In vivo cPAC expression in a *cya*⁻ *E. coli* strain

cPAC and variants in PCB-producing *E. coli* K12 strain VJS711 that lacked the endogenous adenylyl cyclase gene (referred to in this paper as strain *cya*⁻) were grown overnight in LB medium containing 0.2 mM kanamycin and 0.2 mM chloramphenicol in darkness at 30 °C before suspension culture or plate assays. For suspension culture assay, aliquots (3 ml) of the overnight suspension cultures were then transferred to NUNC 12-well cell culture plates (catalog number 150628). To generate Bc, Gc, or continuous red light (Rc) conditions, half of each plate was covered with filters (number 071 Tokyo blue (maximum absorbance: 440 nm) or number 090 dark yellow (maximum absorbance: 525 nm) or number 164 flame red (maximum absorbance: 625 nm) respectively; LEE filters, Burbank, CA) and allowed to incubate further for 6 h. The light fluence rate for light incubation was 4–5 μmol m⁻² s⁻¹. *E. coli* liquid suspension cultures were then analyzed for global cAMP levels with the cAMP Direct EIA kit (Arbor Assays LLC, catalog number K019-H1) as directed by manufacturer. All experiments were performed in triplicate with two technical replicates. The limit of detection of the EIA kit was 0.2 pmol/ml with sensitivity of 0.64 pmol/ml. For plate assays, overnight grown cells were plated on LB plates containing 1 mM IPTG, 84 mg/liter of amino levulinic acid, 0.2 mM kanamycin, and 0.2 mM chloramphenicol to which X-Gal (40 μl) was freshly added. Plates were incubated at 30 °C overnight with light conditions acquired as stated above.

Construction of fusion proteins and site-directed mutagenesis

Synthetic fusion proteins were constructed using a modified protocol for the sequence and ligation-independent cloning method (84). Site-directed mutagenesis was performed using a protocol modified from the QuikChange Site-directed Mutagenesis kit (Agilent Technologies®). Proteins were expressed and analyzed as described above.

Alignment of sequences

Alignments for the cPAC enzyme active site and GAF region were analyzed using MUSCLE (default settings), visualized via JalView, and manually edited in Adobe Illustrator.

Author contributions—M. B.-H., N. C. R., and J. C. L. conceptualization; M. B.-H., N. C. R., M. V. M., S. S. M., F. G., and D. A. B. resources; M. B.-H., N. C. R., D. A. B., and J. C. L. data curation; M. B.-H., N. C. R., and J. C. L. formal analysis; M. B.-H., N. C. R., M. V. M., and S. S. M. validation; M. B.-H., N. C. R., M. V. M., and F. G. investigation; M. B.-H., N. C. R., and J. C. L. visualization; M. B.-H., N. C. R., M. V. M., and S. S. M. methodology; M. B.-H. writing-original draft; M. B.-H., N. C. R., M. V. M., F. G., D. A. B., and J. C. L. writing-review and editing; N. C. R., S. S. M., D. A. B., and J. C. L. supervision; N. C. R., D. A. B., and J. C. L. funding acquisition; S. S. M. project administration.

Acknowledgment—We acknowledge Dr. Valley Stewart (UC Davis) for the gift of the *cya⁻ E. coli VSJ711* strain.

References

- Botsford, J. L., and Harman, J. G. (1992) Cyclic AMP in prokaryotes. *Microbiol. Rev.* **56**, 100–122 [Medline](#)
- Görke, B., and Stülke, J. (2008) Carbon catabolite repression in bacteria: many ways to make the most out of nutrients. *Nat. Rev. Microbiol.* **6**, 613–624 [CrossRef Medline](#)
- Gomelsky, M. (2011) cAMP, c-di-GMP, c-di-AMP and now cGMP: bacteria use them all!. *Mol. Microbiol.* **79**, 562–565 [CrossRef Medline](#)
- Lefkimiatis, K., and Zaccolo, M. (2014) cAMP signaling in subcellular compartments. *Pharmacol. Ther.* **143**, 295–304 [Medline](#)
- Linder, J. U. (2006) Class III adenylyl cyclases: molecular mechanisms of catalysis and regulation. *Cell. Mol. Life Sci.* **63**, 1736–1751 [CrossRef Medline](#)
- Ohmori, K., Hirose, M., and Ohmori, M. (1993) An increase in the intracellular concentration of cAMP triggers formation of an algal mat by the cyanobacterium *Spirulina platensis*. *Plant Cell Physiol.* **34**, 169–171
- Terauchi, K., and Ohmori, M. (1999) An adenylate cyclase, Cya1, regulates cell motility in the cyanobacterium *Synechocystis* sp. PCC 6803. *Plant Cell Physiol.* **40**, 248–251 [CrossRef Medline](#)
- Bhaya, D. (2004) Light matters: phototaxis and signal transduction in unicellular cyanobacteria. *Mol. Microbiol.* **53**, 745–754 [CrossRef Medline](#)
- Smith, G., and Ownby, J. D. (1981) Cyclic AMP interferes with pattern formation in the cyanobacterium *Anabaena variabilis*. *FEMS Microbiol. Lett.* **11**, 175–180 [CrossRef](#)
- Raffelberg, S., Wang, L., Gao, S., Losi, A., Gärtner, W., and Nagel, G. (2013) A LOV-domain-mediated blue-light-activated adenylate (adenylyl) cyclase from the cyanobacterium *Microcoleus chthonoplastes* PCC 7420. *Biochem. J.* **455**, 359–365 [CrossRef Medline](#)
- Ohki, M., Sugiyama, K., Kawai, F., Tanaka, H., Nihei, Y., Unzai, S., Takebe, M., Matsunaga, S., Adachi S-i., and Shibayama, N. (2016) Structural insight into photoactivation of an adenylate cyclase from a photosynthetic cyanobacterium. *Proc. Natl. Acad. Sci. U.S.A.* **113**, 6659–6664 [CrossRef](#)
- Ohmori, M., and Okamoto, S. (2004) Photoresponsive cAMP signal transduction in cyanobacteria. *Photochem. Photobiol. Sci.* **3**, 503–511 [CrossRef](#)
- Okamoto, S., Kasahara, M., Kamiya, A., Nakahira, Y., and Ohmori, M. (2004) A phytochrome-like protein AphC triggers the cAMP signaling induced by far-red light in the cyanobacterium *Anabaena* sp. strain PCC7120. *Photochem. Photobiol.* **80**, 429–433 [Medline](#)
- Rockwell, N. C., and Lagarias, J. C. (2010) A brief history of phytochromes. *Chemphyschem* **11**, 1172–1180 [CrossRef Medline](#)
- Ikeuchi, M., and Ishizuka, T. (2008) Cyanobacteriochromes: a new superfamily of tetrapyrrole-binding photoreceptors in cyanobacteria. *Photochem. Photobiol. Sci.* **7**, 1159–1167 [Medline](#)
- Ho, M. Y., Soulier, N. T., Canniffe, D. P., Shen, G., and Bryant, D. A. (2017) Light regulation of pigment and photosystem biosynthesis in cyanobacteria. *Curr. Opin. Plant Biol.* **37**, 24–33 [CrossRef Medline](#)
- Ishizuka, T., Kamiya, A., Suzuki, H., Narikawa, R., Noguchi, T., Kohchi, T., Inomata, K., and Ikeuchi, M. (2011) The cyanobacteriochrome, TePixJ, isomerizes its own chromophore by converting phycocyanobilin to phycoviolobilin. *Biochemistry* **50**, 953–961 [CrossRef Medline](#)
- Rockwell, N. C., Martin, S. S., Feoktistova, K., and Lagarias, J. C. (2011) Diverse two-cysteine photocycles in phytochromes and cyanobacteriochromes. *Proc. Natl. Acad. Sci. U.S.A.* **108**, 11854–11859 [CrossRef](#)
- Rockwell, N. C., Martin, S. S., Gulevich, A. G., and Lagarias, J. C. (2012) Phycoviolobilin formation and spectral tuning in the DXCF cyanobacteriochrome subfamily. *Biochemistry* **51**, 1449–1463 [CrossRef Medline](#)
- Rockwell, N. C., Martin, S. S., and Lagarias, J. C. (2012) Red/green cyanobacteriochromes: sensors of color and power. *Biochemistry* **51**, 9667–9677 [CrossRef Medline](#)
- Ma, Q., Hua, H. H., Chen, Y., Liu, B. B., Krämer, A. L., Scheer, H., Zhao, K. H., and Zhou, M. (2012) A rising tide of blue-absorbing biliprotein photoreceptors: characterization of seven such bilin-binding GAF domains in *Nostoc* sp. PCC7120. *Febs J.* **279**, 4095–4108 [CrossRef Medline](#)
- Hirose, Y., Rockwell, N. C., Nishiyama, K., Narikawa, R., Ukaji, Y., Inomata, K., Lagarias, J. C., and Ikeuchi, M. (2013) Green/red cyanobacteriochromes regulate complementary chromatic acclimation via a protochromic photocycle. *Proc. Natl. Acad. Sci. U.S.A.* **110**, 4974–4979 [CrossRef](#)
- Enomoto, G., Narikawa, R., and Ikeuchi, M. (2015) Three cyanobacteriochromes work together to form a light color-sensitive input system for c-di-GMP signaling of cell aggregation. *Proc. Natl. Acad. Sci. U.S.A.* **112**, 8082–8087 [CrossRef](#)
- Narikawa, R., Fushimi, K., Win, N. N., and Ikeuchi, M. (2015) Red-shifted red/green-type cyanobacteriochrome AM1_1870g3 from the chlorophyll *d*-bearing cyanobacterium *Acaryochloris marina*. *Biochem. Biophys. Res. Commun.* **461**, 390–395 [CrossRef](#)
- Fushimi, K., Rockwell, N. C., Enomoto, G., Ni-Ni, W., Martin, S. S., Gan, F., Bryant, D. A., Ikeuchi, M., Lagarias, J. C., and Narikawa, R. (2016) Cyanobacteriochrome photoreceptors lacking the canonical Cys residue. *Biochemistry* **55**, 6981–6995 [CrossRef Medline](#)
- Rockwell, N. C., Martin, S. S., and Lagarias, J. C. (2016) Identification of cyanobacteriochromes detecting far-red light. *Biochemistry* **55**, 3907–3919 [CrossRef Medline](#)
- Freer, L. H., Kim, P. W., Corley, S. C., Rockwell, N. C., Zhao, L., Thibert, A. J., Lagarias, J. C., and Larsen, D. S. (2012) Chemical inhomogeneity in the ultrafast dynamics of the DXCF cyanobacteriochrome Tlr0924. *J. Phys. Chem. B* **116**, 10571–10581 [CrossRef](#)
- Iseki, M., Matsunaga, S., Murakami, A., Ohno, K., Shiga, K., Yoshida, K., Sugai, M., Takahashi, T., Hori, T., and Watanabe, M. (2002) A blue-light-activated adenylyl cyclase mediates photoavoidance in *Euglena gracilis*. *Nature* **415**, 1047–1051 [CrossRef Medline](#)
- Schröder-Lang, S., Schwärzel, M., Seifert, R., Strünker, T., Kateriya, S., Looser, J., Watanabe, M., Kaupp, U. B., Hegemann, P., and Nagel, G. (2007) Fast manipulation of cellular cAMP level by light *in vivo*. *Nat. Methods* **4**, 39–42 [CrossRef Medline](#)
- Ryu, M.-H., Moskvina, O. V., Siltberg-Liberles, J., and Gomelsky, M. (2010) Natural and engineered photoactivated nucleotidyl cyclases for optogenetic applications. *J. Biol. Chem.* **285**, 41501–41508 [CrossRef](#)
- Stierl, M., Stumpf, P., Udvari, D., Gueta, R., Hagedorn, R., Losi, A., Gärtner, W., Petereit, L., Efetova, M., and Schwarzel, M. (2011) Light modulation of cellular cAMP by a small bacterial photoactivated adenylyl cyclase, bPAC, of the soil bacterium *Beggiatoa*. *J. Biol. Chem.* **286**, 1181–1188 [CrossRef](#)
- Penzkofer, A., Stierl, M., Hegemann, P., and Kateriya, S. (2011) Photo-dynamics of the BLUF domain containing soluble adenylate cyclase (nPAC) from the amoeboid flagellate *Naegleria gruberi* NEG-M strain. *Chem. Phys.* **387**, 25–38 [CrossRef](#)
- Penzkofer, A., Tanwar, M., Veetil, S. K., Kateriya, S., Stierl, M., and Hegemann, P. (2013) Photo-dynamics and thermal behavior of the BLUF domain containing adenylate cyclase NgPAC2 from the amoeboid flagellate *Naegleria gruberi* NEG-M strain. *Chem. Phys.* **412**, 96–108 [CrossRef](#)
- Penzkofer, A., Tanwar, M., Veetil, S. K., Kateriya, S., Stierl, M., and Hegemann, P. (2014) Photo-dynamics of BLUF domain containing adenylyl cyclase NgPAC3 from the amoeboid flagellate *Naegleria gruberi* NEG-M strain. *J. Photochem. Photobiol. A Chem.* **287**, 19–29 [CrossRef](#)
- Penzkofer, A., Tanwar, M., Veetil, S. K., and Kateriya, S. (2014) Photo-dynamics of photoactivated adenylyl cyclase LiPAC from the spirochete bacterium *Leptonema illini* strain 3055T. *Trends Appl. Spectrometry* **11**, 39–62

Cyanobacterial photoactivatable adenylyl cyclases

36. Penzkofer, A., Tanwar, M., Veetil, S. K., and Kateriya, S. (2015) Photo-dynamics of photoactivated adenylyl cyclase TpPAC from the spirochete bacterium *Turneriella parva* strain H(T). *J. Photochem. Photobiol. B Biol.* **153**, 90–102 [CrossRef](#)
37. Ohki, M., Sato-Tomita, A., Matsunaga, S., Iseki, M., Tame, J. R., Shibayama, N., and Park, S.-Y. (2017) Molecular mechanism of photoactivation of a light-regulated adenylyl cyclase. *Proc. Natl. Acad. Sci. U.S.A.* **114**, 8562–8567 [CrossRef](#)
38. Lindner, R., Hartmann, E., Tarnawski, M., Winkler, A., Frey, D., Reinstein, J., Meinhart, A., and Schlichting, I. (2017) Photoactivation mechanism of a bacterial light-regulated adenylyl cyclase. *J. Mol. Biol.* **429**, 1336–1351 [CrossRef](#) [Medline](#)
39. Ryu, M.-H., Kang, I.-H., Nelson, M. D., Jensen, T. M., Lyuksyutova, A. I., Siltberg-Liberles, J., Raizen, D. M., and Gomelsky, M. (2014) Engineering adenylyl cyclases regulated by near-infrared window light. *Proc. Natl. Acad. Sci. U.S.A.* **111**, 10167–10172 [CrossRef](#)
40. Gambetta, G. A., and Lagarias, J. C. (2001) Genetic engineering of phytochrome biosynthesis in bacteria. *Proc. Natl. Acad. Sci. U.S.A.* **98**, 10566–10571 [CrossRef](#)
41. Rockwell, N. C., Njuguna, S. L., Roberts, L., Castillo, E., Parson, V. L., Dwojak, S., Lagarias, J. C., and Spiller, S. C. (2008) A second conserved GAF domain cysteine is required for the blue/green photoreversibility of cyanobacteriochrome Tlr0924 from *Thermosynechococcus elongatus*. *Biochemistry* **47**, 7304–7316 [Medline](#)
42. Rockwell, N. C., Martin, S. S., and Lagarias, J. C. (2012) Mechanistic insight into the photosensory versatility of DXCF cyanobacteriochromes. *Biochemistry* **51**, 3576–3585 [CrossRef](#) [Medline](#)
43. Shenoy, A. R., and Visweswariah, S. S. (2004) Class III nucleotide cyclases in bacteria and archaeobacteria: lineage-specific expansion of adenylyl cyclases and a dearth of guanylyl cyclases. *FEBS Lett.* **561**, 11–21 [CrossRef](#) [Medline](#)
44. Oliveira, M. C., Teixeira, R. D., Andrade, M. O., Pinheiro, G. M., Ramos, C. H., and Farah, C. S. (2015) Cooperative substrate binding by a diguanylate cyclase. *J. Mol. Biol.* **427**, 415–432 [CrossRef](#) [Medline](#)
45. Yang, J. K., and Epstein, W. (1983) Purification and characterization of adenylyl cyclase from *Escherichia coli* K12. *J. Biol. Chem.* **258**, 3750–3758 [Medline](#)
46. Galperin, M. Y. (2006) Structural classification of bacterial response regulators: diversity of output domains and domain combinations. *J. Bacteriol.* **188**, 4169–4182 [CrossRef](#) [Medline](#)
47. Bourret, R. B. (2010) Receiver domain structure and function in response regulator proteins. *Curr. Opin. Microbiol.* **13**, 142–149 [CrossRef](#) [Medline](#)
48. Okkotsu, Y., Tiekou, P., Fitzsimmons, L. F., Churchill, M. E., and Schurr, M. J. (2013) *Pseudomonas aeruginosa* AlgR phosphorylation modulates rhamnolipid production and motility. *J. Bacteriol.* **195**, 5499–5515 [CrossRef](#) [Medline](#)
49. Aldridge, P., Paul, R., Goymer, P., Rainey, P., and Jenal, U. (2003) Role of the GGDEF regulator PleD in polar development of *Caulobacter crescentus*. *Mol. Microbiol.* **47**, 1695–1708 [CrossRef](#) [Medline](#)
50. Klose, K. E., Weiss, D. S., and Kustu, S. (1993) Glutamate at the site of phosphorylation of nitrogen-regulatory protein NTRC mimics aspartyl-phosphate and activates the protein. *J. Mol. Biol.* **232**, 67–78 [CrossRef](#) [Medline](#)
51. Huynh, T. N., Chen, L.-L., and Stewart, V. (2015) Sensor–response regulator interactions in a cross-regulated signal transduction network. *Microbiology* **161**, 1504–1515 [CrossRef](#) [Medline](#)
52. Fushimi, K., Ikeuchi, M., and Narikawa, R. (2017) The expanded red/green cyanobacteriochrome lineage: an evolutionary hot spot. *Photochem. Photobiol.* **93**, 903–906 [CrossRef](#) [Medline](#)
53. Tabor, J. J., Levskaya, A., and Voigt, C. A. (2011) Multichromatic control of gene expression in *Escherichia coli*. *J. Mol. Biol.* **405**, 315–324 [CrossRef](#) [Medline](#)
54. Ramakrishnan, P., and Tabor, J. J. (2016) Repurposing *Synechocystis* PCC6803 UirS–UirR as a UV-violet/green photoreversible transcriptional regulatory tool in *E. coli*. *ACS Synth. Biol.* **5**, 733–740 [CrossRef](#) [Medline](#)
55. Fushimi, K., Enomoto, G., Ikeuchi, M., and Narikawa, R. (2017) Distinctive properties of dark reversion kinetics between two red/green-type cyanobacteriochromes and their application in the photoregulation of cAMP synthesis. *Photochem. Photobiol.* **93**, 681–691 [CrossRef](#) [Medline](#)
56. Gan, F., Zhang, S., Rockwell, N. C., Martin, S. S., Lagarias, J. C., and Bryant, D. A. (2014) Extensive remodeling of a cyanobacterial photosynthetic apparatus in far-red light. *Science* **345**, 1312–1317 [CrossRef](#) [Medline](#)
57. Jørgensen, B. B., Cohen, Y., and Revsbech, N. P. (1986) Transition from anoxygenic to oxygenic photosynthesis in a *Microcoleus chthonoplastes* cyanobacterial mat. *Appl. Environ. Microbiol.* **51**, 408–417 [Medline](#)
58. Karsten, U., and Garcia-Pichel, F. (1996) Carotenoids and mycosporine-like amino acid compounds in members of the genus *Microcoleus* (Cyanobacteria): a chemosystematic study. *Syst. Appl. Microbiol.* **19**, 285–294 [CrossRef](#)
59. Omoregie, E. O., Crumbliss, L. L., Bebout, B. M., and Zehr, J. P. (2004) Determination of nitrogen-fixing phylotypes in Lyngbya sp., and *Microcoleus chthonoplastes* cyanobacterial mats from Guerrero Negro, Baja California, Mexico. *Appl. Environ. Microbiol.* **70**, 2119–2128 [CrossRef](#) [Medline](#)
60. Gordillo, F. J., Segovia, M., and López-Figueroa, F. (2004) Cyclic AMP levels in several macroalgae and their relation to light quantity and quality. *J. Plant Physiol.* **161**, 211–217 [CrossRef](#) [Medline](#)
61. Hegemann, P. (2008) Algal sensory photoreceptors. *Annu. Rev. Plant Biol.* **59**, 167–189 [CrossRef](#) [Medline](#)
62. Penzkofer, A., Kateriya, S., and Hegemann, P. (2016) Photodynamics of the optogenetic BLUF coupled photoactivated adenylyl cyclases (PACs). *Dyes Pigments* **135**, 102–112 [CrossRef](#)
63. Enomoto, G., Nomura, R., Shimada, T., Narikawa, R., and Ikeuchi, M. (2014) Cyanobacteriochrome SesA is a diguanylate cyclase that induces cell aggregation in *Thermosynechococcus*. *J. Biol. Chem.* **289**, 24801–24809 [CrossRef](#)
64. Mulder, D. T., McPhee, J. B., Reid-Yu, S. A., Stogios, P. J., Savchenko, A., and Coombes, B. K. (2015) Multiple histidines in the periplasmic domain of the *Salmonella enterica* sensor kinase SsrA enhance signaling in response to extracellular acidification. *Mol. Microbiol.* **95**, 678–691 [CrossRef](#) [Medline](#)
65. Chen, Y., Cann, M. J., Litvin, T. N., Iourgenko, V., Sinclair, M. L., Levin, L. R., and Buck, J. (2000) Soluble adenylyl cyclase as an evolutionarily conserved bicarbonate sensor. *Science* **289**, 625–628 [CrossRef](#) [Medline](#)
66. Cann, M. J., Hammer, A., Zhou, J., and Kanacher, T. (2003) A defined subset of adenylyl cyclases is regulated by bicarbonate ion. *J. Biol. Chem.* **278**, 35033–35038 [CrossRef](#)
67. Kobayashi, M., Buck, J., and Levin, L. R. (2004) Conservation of functional domain structure in bicarbonate-regulated “soluble” adenylyl cyclases in bacteria and eukaryotes. *Dev. Genes Evol.* **214**, 503–509 [Medline](#)
68. Litvin, T. N., Kamenetsky, M., Zarifyan, A., Buck, J., and Levin, L. R. (2003) Kinetic properties of “soluble” adenylyl cyclase synergism between calcium and bicarbonate. *J. Biol. Chem.* **278**, 15922–15926 [CrossRef](#)
69. Steegborn, C., Litvin, T. N., Levin, L. R., Buck, J., and Wu, H. (2005) Bicarbonate activation of adenylyl cyclase via promotion of catalytic active site closure and metal recruitment. *Nat. Struct. Mol. Biol.* **12**, 32–37 [CrossRef](#) [Medline](#)
70. Rockwell, N. C., and Lagarias, J. C. (2017) Ferredoxin-dependent bilin reductases in eukaryotic algae: ubiquity and diversity. *J. Plant Physiol.* **217**, 57–67 [CrossRef](#) [Medline](#)
71. Duanmu, D., Casero, D., Dent, R. M., Gallaher, S., Yang, W., Rockwell, N. C., Martin, S. S., Pellegrini, M., Niyogi, K. K., Merchant, S. S., Grossman, A. R., and Lagarias, J. C. (2013) Retrograde bilin signaling enables *Chlamydomonas* greening and phototrophic survival. *Proc. Natl. Acad. Sci. U.S.A.* **110**, 3621–3626 [CrossRef](#) [Medline](#)
72. Yoshikawa, S., Suzuki, T., Watanabe, M., and Iseki, M. (2005) Kinetic analysis of the activation of photoactivated adenylyl cyclase (PAC), a blue-light receptor for photomovements of *Euglena*. *Photochem. Photobiol. Sci.* **4**, 727–731 [Medline](#)
73. Song, J.-Y., Cho, H. S., Cho, J.-I., Jeon, J.-S., Lagarias, J. C., and Park, Y.-I. (2011) Near-UV cyanobacteriochrome signaling system elicits negative phototaxis in the cyanobacterium *Synechocystis* sp. PCC 6803. *Proc. Natl. Acad. Sci. U.S.A.* **108**, 10780–10785 [CrossRef](#)

74. Lim, S., Rockwell, N. C., Martin, S. S., Dallas, J. L., Lagarias, J. C., and Ames, J. B. (2014) Photoconversion changes bilin chromophore conjugation and protein secondary structure in the violet/orange cyanobacteriochrome NpF2164g3. *Photochem. Photobiol. Sci.* **13**, 951–962 [Medline](#)
75. Müller, K., and Weber, W. (2013) Optogenetic tools for mammalian systems. *Mol. Biosyst.* **9**, 596–608 [CrossRef Medline](#)
76. Shin, A. Y., Han, Y. J., Song, P. S., and Kim, J. I. (2014) Expression of recombinant full-length plant phytochromes assembled with phytochromobilin in *Pichia pastoris*. *FEBS Lett.* **588**, 2964–2970 [CrossRef Medline](#)
77. Uda, Y., Goto, Y., Oda, S., Kohchi, T., Matsuda, M., and Aoki, K. (2017) Efficient synthesis of phycocyanobilin in mammalian cells for optogenetic control of cell signaling. *Proc. Natl. Acad. Sci. U.S.A.* **114**, 11962–11967 [CrossRef](#)
78. Kyriakakis, P., Catanho, M., Hoffner, N., Thavarajah, W., Hu, V. J., Chao, S. S., Hsu, A., Pham, V., Naghavian, L., Dozier, L. E., Patrick, G. N., and Coleman, T. P. (2018) Biosynthesis of orthogonal molecules using ferredoxin and ferredoxin-NADP⁺ reductase systems enables genetically encoded phyB optogenetics. *ACS Synth. Biol.* **7**, 706–717 [CrossRef Medline](#)
79. Ong, N. T., Olson, E. J., and Tabor, J. J. (2018) Engineering an *E. coli* near-infrared light sensor. *ACS Synth. Biol.* **7**, 240–248 [CrossRef Medline](#)
80. Shemetov, A. A., Oliinyk, O. S., and Verkhusha, V. V. (2017) How to increase brightness of near-infrared fluorescent proteins in mammalian cells. *Cell Chem. Biol.* **24**, 758–766.e3 [CrossRef Medline](#)
81. Ryu, M. H., Fomicheva, A., Moskvin, O. V., and Gomelsky, M. (2017) Optogenetic module for dichromatic control of c-di-GMP signaling. *J. Bacteriol.* **199**, pii: e00014–00017 [Medline](#)
82. Gasser, C., Taiber, S., Yeh, C.-M., Wittig, C. H., Hegemann, P., Ryu, S., Wunder, F., and Möglich, A. (2014) Engineering of a red-light-activated human cAMP/cGMP-specific phosphodiesterase. *Proc. Natl. Acad. Sci. U.S.A.* **111**, 8803–8808 [CrossRef](#)
83. Blain-Hartung, M., Rockwell, N. C., and Lagarias, J. C. (2017) Light-regulated synthesis of cyclic-di-GMP by a bidomain construct of the cyanobacteriochrome Tlr0924 (SesA) without stable dimerization. *Biochemistry* **56**, 6145–6154 [CrossRef Medline](#)
84. Li, M. Z., and Elledge, S. J. (2012) SLIC: a method for sequence-and ligation-independent cloning. *Methods Mol. Biol.* **852**, 51–59 [CrossRef Medline](#)